Chirped Microwave Pulse Generation Based on Optical Spectral Shaping and Wavelength-to-Time Mapping Using a Sagnac Loop Mirror Incorporating a Chirped Fiber Bragg Grating

Chao Wang, *Student Member, IEEE*, and Jianping Yao, *Senior Member, IEEE*

***Abstract*—In this paper, we propose and demonstrate an approach to optically generating chirped microwave pulses with tunable chirp profile based on optical spectral shaping using a Sagnac loop filter incorporating a chirped fiber Bragg grating (CFBG) and linear wavelength-to-time mapping in a dispersive element. In the proposed approach, the optical power spectrum of an ultrashort optical pulse is shaped by a CFBG-incorporated Sagnac loop mirror that has a reflection spectral response with a linearly increasing or decreasing free spectral range. The spectrum-shaped optical pulse is then sent to a dispersive element to perform the linear wavelength-to-time mapping. A chirped microwave pulse with the pulse shape identical to that of the shaped spectrum is obtained at the output of a high-speed photodector. The central frequency and the chirp profile of the generated chirped microwave pulse can be controlled by simply tuning the time delay in the Sagnac loop mirror. A simple mathematical model to describe the chirped microwave pulse generation is developed. Numerical simulations and a proof-of-principle experiment are implemented to verify the proposed approach.**

***Index Terms*—Chirped microwave pulse, dispersion, fiber Bragg grating (FBG), optical pulse shaping, Sagnac loop mirror, wavelength-to-time mapping.**

I. Introduction

MICROWAVE pulse compression has been extensively employed in modern radar systems, where the transmitted signals are usually frequency-chirped or phase-modulated to increase the time-bandwidth product (TBWP), leading to an increased radar range resolution and detection distance [1]. Chirped microwave pulses are conventionally generated in the electrical domain based on electronic circuitry [2], [3] but with the limitations of small TBWP and low central frequency. At the current stage of development of a radar system, the central frequency up to tens or even hundreds of GHz is often required [1]. As a promising alternative, photonic generation of microwave pulses has been an active topic, thanks to the broad bandwidth and high speed offered by optics. Various approaches to generating microwave and millimeter-wave waveforms with arbitrary pulse shape in the optical domain have been proposed, such as those based on frequency-domain pulse shaping [4]–[6], temporal pulse shaping (TPS) [7]–[9], and direct space-to-time mapping [10]–[14]. Recently, an all-optical method to generate linearly chirped microwave pulses based on the interference of two chromatically dispersed optical pulses in a Mach--Zehnder interferometer was demonstrated [15]. The optical pulses are obtained by passing a broadband ultrashort pulse through two chirped fiber Bragg gratings (CFBGs) with different chirp rates. The beating of the two time-delayed dispersed optical pulses leads to the generation of a chirped microwave pulse.

Optical spectral shaping followed by wavelength-to-time mapping in a dispersive element has also been demonstrated to be a promising technique to generate arbitrary microwave waveforms [16]–[23], in which a temporal microwave pulse with a shape identical to the shaped spectrum can be generated. In an optical spectral shaping system, a spatial light modulator (SLM) [19]–[21] or a fiber-optic spectral filter [22], [23] is usually used to shape the optical spectrum of an ultrashort pulse. The key advantage of the SLM-based technique is the high degree of controllability and real-time updatability. The major difficulty associated with the SLM-based technique is that the spectral shaping is implemented in free space, which requires fiber-to-space and space-to-fiber coupling, making the system bulky, lossy, and complicated. An all-fiber filter could be used to realize optical spectrum shaping to take advantage of the features such as low loss, small size, and high potential for integration.

Photonic generation of chirped microwave pulses based on spectral shaping using a fiber-optic filter and wavelength-to-time mapping in a dispersive element have been recently demonstrated [24]–[27]. By using an optical filter with a uniform free spectral range (FSR), along with a dispersive device having both the first- and second-order dispersions, chirped microwave or millimeter-wave pulses were generated, thanks to the nonlinear wavelength-to-time mapping in the higher-order dispersive element, such as a nonlinearly CFBG [24], [25] or a higher-order dispersive fiber [26]. Chirped microwave pulses can also be generated based on spectral shaping using an optical filter with a varying FSR, followed by linear wavelength-to-time mapping. An optical filter with varying FSR was recently demonstrated by using two superimposed CFBGs in a single fiber [27]. Since

Manuscript received September 15, 2008; revised November 24, 2008. First published April 17, 2009; current version published July 24, 2009. This work was supported by the Natural Science and Engineering Research Council of Canada (NSERC).

The authors are with the Microwave Photonics Research Laboratory, School of Information Technology and Engineering, University of Ottawa, ON K1N 6N5, Canada (e-mail: jpyao@site.uottawa.ca).

Color versions of one or more of the figures in this paper are available online at http://ieeexplore.ieee.org.

Digital Object Identifier 10.1109/JLT.2008.2010561

the two CFBGs need to be written in a single fiber, the fabricated process is complicated. In addition, the longitudinal offset between the two CFBGs is fixed once the two CFBGs are fabricated; therefore, the central frequency and the chirp profile of the generated chirped microwave pulse cannot be tuned.

In this paper, we propose and demonstrate a simple approach to optically generating chirped microwave pulses based on spectral shaping using a novel optical filter with a varying FSR and wavelength-to-time mapping in a linear dispersive element. The spectral filter is a CFBG-incorporated Sagnac loop mirror having a spectral response with linearly increasing or decreasing FSR. A linearly chirped microwave pulse can be generated after the linear wavelength-to-time mapping.

A Sagnac loop mirror incorporating a uniform FBG with a constant FSR has been proposed for applications such as in a multiwavelength fiber laser [28]. To the best of our knowledge, however, this is the first time that a CFBG-incorporated Sagnac loop mirror with a varying FSR is employed to generate chirped microwave pulses. Since only one linearly CFBG is needed, the proposed filter, compared with the approach in [27], has the advantages of simpler configuration and lower insertion loss. In addition, by tuning the time delay in the Sagnac loop mirror, the central frequency and the sign of chirp rate of the generated chirped microwave pulses can be controlled.

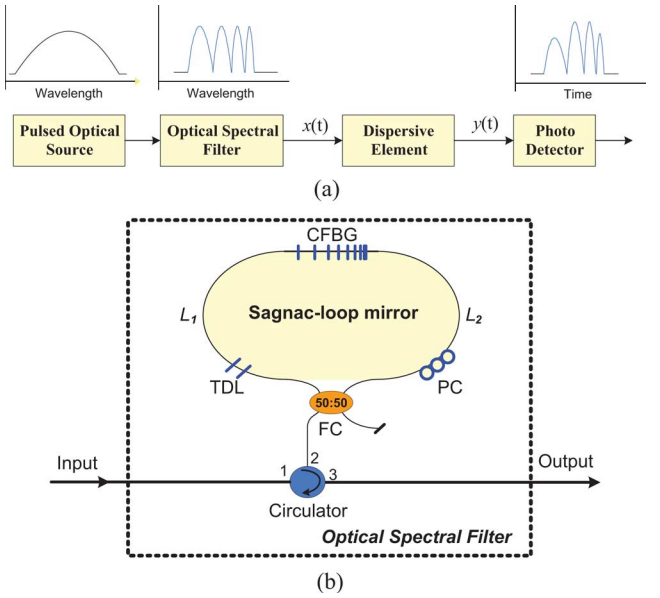

Fig. 1. (a) Schematic diagram showing a microwave pulse generation system based on optical spectral shaping and dispersion-induced wavelength-to-time mapping. (b) All-fiber optical spectral filter based on CFBG-incorporated Sagnac loop mirror. FC: fiber coupler; TDL: tunable delay-line; CFBG: chirped fiber Bragg grating; PC: polarization controller.

II. Principle

It is known that a dispersive element, such as a length of dispersive fiber or a CFBG, can be modeled as a linear time-invariant system with a transfer function given by $H(\omega) = |H(\omega)|\exp[-j\Phi(\omega)]$. When a transform-limited ultrashort optical pulse $x(t)$ is sent to the dispersion element, under first-order dispersion approximation, the output dispersed pulse $y(t)$ can be obtained according to the so-called time-domain Fraunhofer diffraction [17]

$$y(t) \approx \exp\left(j\frac{1}{2\ddot{\Phi}}t^2\right) X(\omega)|_{\omega=2\pi t/\ddot{\Phi}} \tag{1}$$

where $X(\omega) = \tilde{F}[x(t)]$ is the Fourier transform of the input pulse $x(t)$, and $\ddot{\Phi} = d^2\Phi(\omega)/d\omega^2|_{\omega=\omega_0}$ is the first-order dispersion coefficient of the dispersive element. It is shown in (1) that the output temporal pulse envelope is proportional to the spectrum envelope of the input pulse with a phase factor and, therefore, the dispersion-induced linear frequency-to-time mapping is obtained. The mapping relationship is given by $\omega = (2\pi/\ddot{\Phi}_v)t$ or $\lambda = (1/1\ddot{\Phi}_\lambda)t$, where $\ddot{\Phi}_v(\text{ps}^2)$ or $\ddot{\Phi}_\lambda$ (ps/nm) is the first-order dispersion coefficient ($\ddot{\Phi}_v = (\lambda^2/c)\ddot{\Phi}_\lambda$).

Therefore, the TPS can be performed in the frequency domain, which is easy to implement using an optical spectral filter. The schematic diagram of the proposed system for microwave pulse generation based on optical spectral shaping and frequency-to-time mapping is shown in Fig. 1(a). A transform-limited broadband ultrashort optical pulse generated by a pulsed optical source is first spectrum shaped by an optical spectral filter. The filter is designed to have a spectral response identical to the shape of the target microwave pulse to be generated. The spectrum-shaped optical pulse is then sent to a dispersive element to perform the linear wavelength-to-time mapping. At the output of a high-speed photodector (PD), a microwave pulse with the shape identical to that of the shaped optical spectrum is obtained.

To generate a linearly chirped microwave pulse, the optical spectral filter should have a linearly increasing or decreasing FSR. In this paper, we introduce an all-fiber optical spectral filter with a linearly varying FSR, which is based on a Sagnac loop mirror with a linearly CFBG incorporated in the fiber loop. Fig. 1(b) shows the schematic of the proposed optical spectral filter based on an all-fiber Sagnac loop mirror. The Sagnac loop mirror is constructed from a fused 3-dB fiber coupler (FC) spliced to the terminals of the CFBG, which is located approximately at the middle point of the fiber loop. A tunable delay-line (TDL) is located in the fiber loop to finely tune the time-delay difference between two fiber lengths L_1 and L_2. A polarization controller is also placed in the loop to adjust the fringe visibility of the interference pattern at the output of the loop. A three-port optical circulator is used to direct the ultrashort pulse into the loop mirror and to output the spectrum-shaped pulse for wavelength-to-time mapping.

Mathematically, the FBG-incorporated Sagnac loop mirror can be modeled as a two-tap delay-line filter. For an all-fiber optical pulse shaping system, it is more convenient to describe the filter response as a function of wavelength. Then, the intensity transfer function of the Sagnac loop mirror is expressed as

$$T(\lambda) = \frac{1}{2}W(\lambda) \times \left[1+\cos\left(\frac{2\pi n_e}{\lambda}2\Delta L\right)\right], \left(|\lambda-\lambda_0| \le \frac{B_\lambda}{2}\right) \tag{2}$$

where $W(\lambda)$ is the intensity reflection spectrum of the CFBG with a bandwidth B_λ, and n_e is the effective refractive index of the fiber core. $\Delta L = L_1 - L_2$ is the fiber length difference, with L_1 and L_2 measured from the center of the CFBG to the FC along the clockwise and counterclockwise paths as shown

in Fig. 1(b). The fiber length difference ΔL comes from two sources: the wavelength-independent path difference ΔL_0 and the wavelength-dependent fiber length difference introduced by the chirp of the CFBG $\Delta L(\lambda)$. ΔL_0 can be controlled to be either a positive or a negative value by tuning the TDL in the fiber loop. $\Delta L(\lambda)$ is determined by the bandwidth and the chirp parameter of the CFBG and can be calculated using $\Delta L(\lambda) = \delta\lambda/C$, where $\delta\lambda$ (nm) is the wavelength detuning from the center wavelength λ_0, and C (nm/cm) is the chirp parameter of the CFBG. Then the filter transfer function $T(\lambda)$ can be rewritten as

$$T(\lambda) \cong \frac{1}{2}W(\lambda)\left[1+\cos\left(\frac{4\pi n_e}{\lambda_0^2}\lambda\left(\Delta L_0+\frac{\delta\lambda}{C}\right)\right)\right]. \quad (3)$$

Since a linearly CFBG is located in the fiber loop, the optical signals with different wavelengths will be reflected from different positions in the CFBG. As a result, an optical spectral filter with a wavelength-dependent FSR is obtained. In other words, an interference fringe pattern is generated within the bandwidth of the CFBG, with a varying FSR due to the chirp of the CFBG. In our analysis, the FSR of the optical spectral filter response, defined as the wavelength separation between two adjacent fringes, is a function of the wavelength λ and can be expressed as

$$\mathrm{FSR} = \frac{\lambda^2}{2n_e|\Delta L|} \cong \frac{\lambda_0^2}{2n_e\left|\frac{\delta\lambda}{C}+\Delta L_0\right|}. \quad (4)$$

According to (4), by properly choosing the parameters of the CFBG and by controlling the TDL in the fiber loop, the FSR of the Sagnac loop-mirror-based optical spectral filter can be controlled. For simplicity, we assume that the input ultrashort optical pulse is a Dirac delta function. Therefore, the intensity spectrum of the shaped optical pulse at the output of the Sagnac loop mirror is identical to the transfer function of the optical spectral filter in (3).

After the spectrum-shaped optical pulse propagates through the dispersive element and is detected by the high-seed PD, the shaped spectrum is mapped into a temporal microwave pulse as $T(\lambda) \rightarrow y(t)$, thanks to the dispersion-induced linear wavelength-to-time mapping. According to the mapping relationship in (1), the converted time-domain waveform is given by

$$y(t) \propto \frac{1}{2}W\left(\frac{t}{\ddot{\Phi}_\lambda}\right)\left\{1+\cos\left[\frac{4\pi n_e}{\lambda_0^2\ddot{\Phi}_\lambda}t\left(\Delta L_0+\frac{\delta t}{C\ddot{\Phi}_\lambda}\right)\right]\right\} \quad (5)$$

where δt is the time detuning from the center of the temporal waveform, which is given by the mapping relationship $\delta\lambda \rightarrow \delta t/\ddot{\Phi}_\lambda$. The time-domain pulse duration of the generated microwave pulse is determined by the window function $W(t/\ddot{\Phi}_\lambda)$ and is calculated by $\Delta T = B_\lambda\ddot{\Phi}_\lambda$. Considering that the pulsewidth of the input ultrashort optical pulse is not zero, the detected pulse envelope should be modified by an envelope $r(t)$

$$y(t) \propto \frac{1}{2} \cdot r(t) \cdot W\left(\frac{t}{\ddot{\Phi}_\lambda}\right)\left\{1+\cos\left[\frac{4\pi n_e}{\lambda_0^2\ddot{\Phi}_\lambda}t(\Delta L_0+\frac{\delta t}{C\ddot{\Phi}_\lambda})\right]\right\} \quad (6)$$

where $r(t)$ is the pulse envelope after the input pulse passing through the dispersive element. Assuming that the input ultrashort optical pulse has a Gaussian envelope as $g(t) \propto \exp(-t^2/t_0^2)$, where t_0 is the half pulsewidth at $1/e$ maximum. Then, the envelope of output pulse from a dispersive element will maintain the Gaussian shape but with a broadened pulsewidth of $\left|\ddot{\Phi}_v\right|/t_0$ [29]. Actually, the envelope $r(t)$ is a scaled version of the spectrum envelope of the input pulse, which is mapped to the time domain, thanks to the dispersion-induced frequency-to-time mapping in the CFBG [17].

The instantaneous microwave carrier frequency of the generated waveform can be obtained from the phase term of (6), which is expressed as

$$f_{\mathrm{RF}}(\delta t) = \frac{1}{2\pi}\cdot\frac{d\Psi}{dt} = \frac{2n_e|\Delta L_0|}{\lambda_0^2\ddot{\Phi}_\lambda} \pm \frac{2n_e\cdot\delta t}{C\lambda_0^2\ddot{\Phi}_\lambda^2}. \quad (7)$$

It is shown that the generated microwave pulse is linearly chirped. For a given dispersive element, the central RF carrier frequency of the generated chirped microwave pulse, defined by $f_{\mathrm{RF}}(\delta t)|_{\delta t=0}$, is only determined by the absolute value of wavelength-independent fiber length difference ΔL_0. In other words, a chirped microwave pulse with a symmetrical, linearly increasing, or decreasing chirp can be generated by simply tuning ΔL_0. The chirp rate of the generated microwave pulse, defined by $R_{\mathrm{RF}} = df_{\mathrm{RF}}(\delta t)/d\delta t = \pm 2n_e/(C\lambda_0^2\ddot{\Phi}_\lambda^2)$, is only dependant upon the chirp parameter of the CFBG. The positive sign and negative sign of the chirp rate correspond to the positive and negative value of ΔL_0, respectively. Therefore, by appropriately controlling the TDL and choosing the chirp parameter of the CFBG, a linearly chirped microwave pulse with a high central frequency and a tunable chirp profile can be generated.

The pulse compression ratio is determined by the TBWP of the transmitted microwave pulse. In our system, the TBWP of the generated chirped microwave pulse is estimated by

$$\mathrm{TBWP} = R_{\mathrm{RF}}\Delta T^2 = 4\frac{n_e}{\lambda_0^2}C\cdot l^2 \quad (8)$$

where l is the length of the CFBG. It is shown that the TBWP is independent of the dispersion in the system but is solely determined by the parameters of the CFBG. For a CFBG with a given chirp parameter, for example, a longer grating leads to a larger TBWP.

In a pulsed radar system, chirped pulse compression is implemented through matched filtering at the receiver end. Mathematically, the matched filtering operation is identical to an autocorrelation operation given by

$$A(t) = y(t) * y(-t) = \int_{-\infty}^{\infty} y(t+\tau)\cdot y(\tau)d\tau \quad (9)$$

where $*$ denotes the convolution operation.

III. Results and Discussion

Numerical simulations and a proof-of-concept experiment are carried out to verify the proposed approach. In the simulations, a transform-limited ultrashort Gaussian pulse with a full-width at half-maximum (FWHM) of 500 fs and with

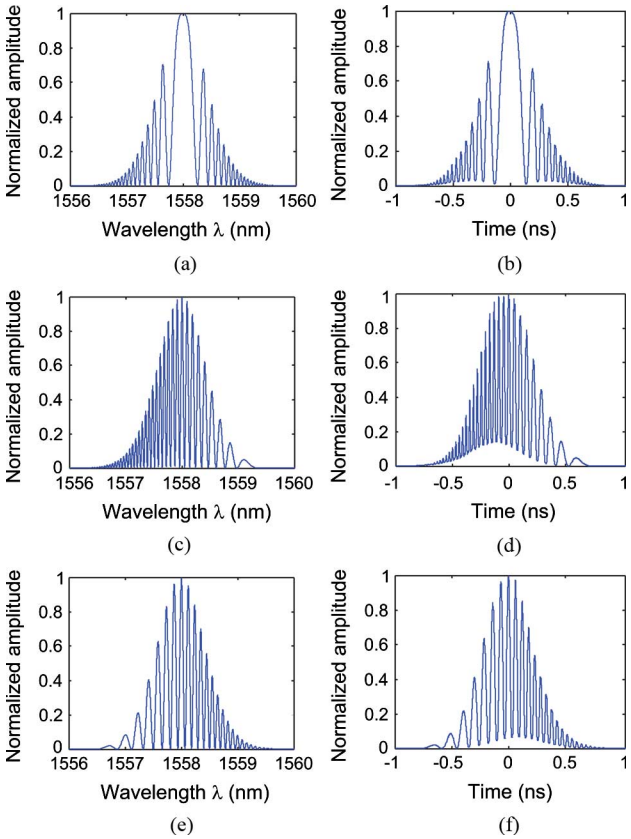

Fig. 2. Simulation results. The intensity spectra of the shaped optical pulse with (a) a symmetrical FSR ($\Delta L_0 = 0$), (c) an increasing FSR ($\Delta L_0 = -9.7$ mm), and (e) a decreasing FSR ($\Delta L_0 = 6.9$ mm). The generated time-domain waveforms with (b) a symmetrical chirp rate and a zero central frequency, (d) a negative chirp rate and a central frequency of 22.3 GHz, and (f) a positive chirp rate and a central frequency of 16.1 GHz.

a central wavelength of 1558 nm is used as the input optical pulse. The CFBG has a length of 1 cm with a chirp rate of 2.0 nm/cm. A proper Gaussian apodization is applied to the CFBG in the simulations. The optical spectral response of the CFBG-incorporated Sagnac loop mirror is calculated according to (3). Different values of ΔL_0 are chosen by tuning the TDL in the fiber loop, leading to the optical spectral response with a symmetrical, monotonically increasing, or monotonically decreasing FSR, as shown in Fig. 2(a), (c), and (e). After the linear wavelength-to-time mapping in a 30.8-km single-mode fiber (SMF) ($\ddot{\Phi}_\lambda = 538\ \mathrm{ps/nm}$), time-domain waveforms with different central frequencies are generated, as shown in Fig. 2(b), (d), and (f). The chirp rates of generated microwave waveforms are $\pm 0.023\ \mathrm{GHz/ps}$, which matches well with the theoretical prediction by (7). Note that the calculated time-domain waveforms have a poorer modulation depth compared with the shaped optical spectra, especially for the cases of small FSR [Figs. 2(c) and (d)]. This is mainly caused by the dispersion mismatch for the specific FSR in the wavelength-to-time mapping process [24].

An experimental demonstration based on the setup shown in Fig. 3 is then implemented to verify the proposed approach for chirped microwave pulse generation. In the experiment, we use a transform-limited ultrashort Gaussian pulse generated from a

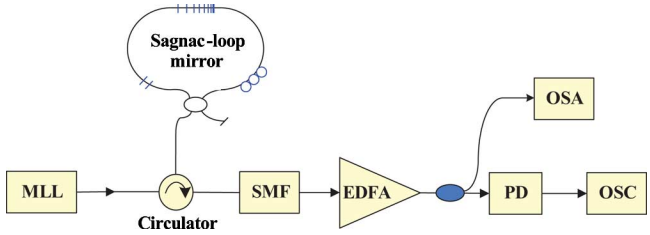

Fig. 3. Schematic diagram showing the generation of chirped microwave pulses based on spectral shaping and linear frequency-to-time conversion. (MLL: mode-locked laser, SMF: single-mode fiber, EDFA: erbium-doped fiber amplifier, OSA: optical spectrum analyzer, PD: photodetector, OSC: oscilloscope).

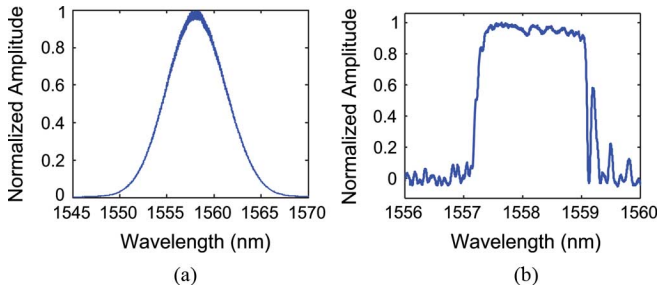

Fig. 4. The optical spectra of (a) input ultrashort pulse and (b) the fabricated CFBG (reflection).

passively mode-locked laser with a FWHM of 550 fs. The central wavelength of the pulse is 1558.3 nm, and the 3-dB spectral bandwidth is 8 nm, as shown in Fig. 4(a). The input pulse is sent to the CFBG-incorporated Sagnac loop mirror. The CFBG is fabricated using a frequency-doubled argon-ion laser operating at 244 nm. The CFBG has a length of 1 cm with a chirp rate of 2.0 nm/cm. To ensure that the light waves are fully reflected by the CFBG in the fiber loop, the fabricated CFBG has a strong reflection as high as 98%. The center Bragg wavelength of the CFBG is 1558.1 nm, which is selected to match the center wavelength of the ultrashort optical pulse. The reflection spectrum of the fabricated CFBG is also shown in Fig. 4(b). The experimental results are measured both in the frequency domain using an optical spectrum analyzer (OSA) with a wavelength resolution of 0.01 nm and in the time domain using a sampling oscilloscope with a bandwidth of 63 GHz.

In the experiment, we first choose the fiber loop to have a positive length difference of $\Delta L_0 = 9.2$ mm by controlling the TDL. Fig. 5(a) shows the measured spectral response of the CFBG-incorporated Sagnac loop mirror. It is shown that an optical spectral filter with a decreasing FSR is obtained, which is then used to spectrally shape the spectrum of the input ultrashort optical pulse. It is worth noting that the measured reflection spectra have a reduced modulation depth. This is mainly caused by the limited resolution of the OSA.

The spectrum of the shaped optical pulse is then mapped to a chirped temporal waveform, thanks to the linear wavelength-to-time mapping in a 30.8-km SMF ($\ddot{\Phi}_\lambda = 538\ \mathrm{ps/nm}$). A positively chirped microwave pulse is experimentally generated, as shown in Fig. 5(b). The dotted line shows the ideal Gaussian pulse envelope. The FWHM of the generated pulse envelope is around 1150 ps. The circles in Fig. 5(c) show the

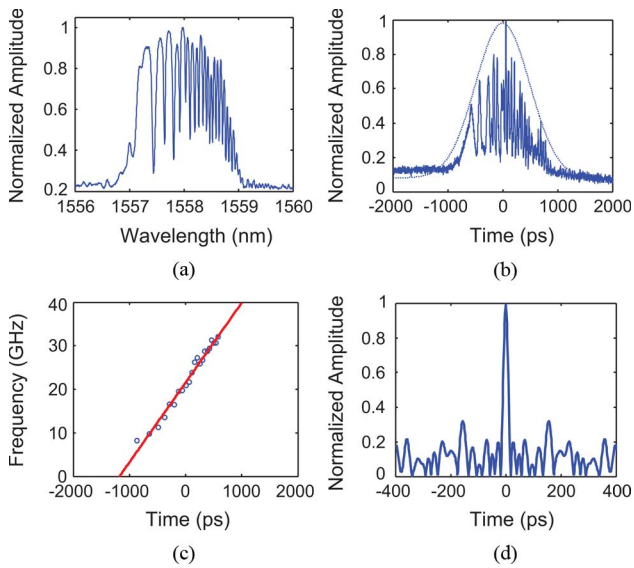

Fig. 5. Experimental results. (a) Spectral response of the Sagnac loop mirror with a decreasing FSR. (b) Generated waveform with a positive chirp rate (dotted line: ideal Gaussian envelope). (c) Instantaneous RF frequency (solid line: linear fitting, circle: obtained from experimental result). (d) Compressed pulse by autocorrelation.

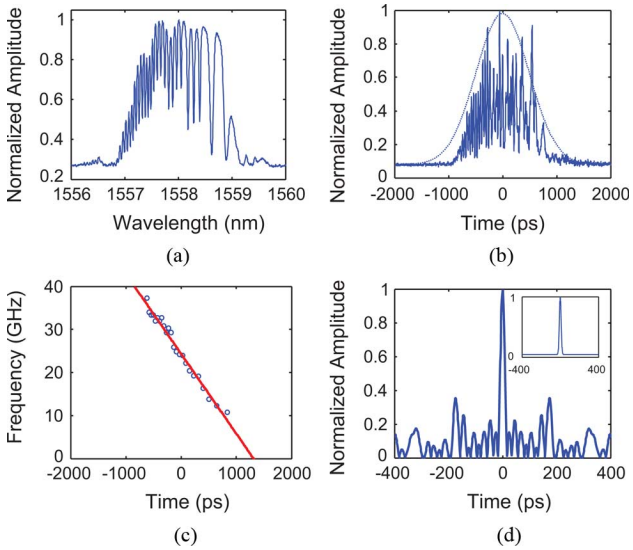

Fig. 6. Experimental results. (a) Spectral response of the Sagnac loop mirror with an increasing FSR. (b) Generated waveform with a negative chirp rate (dotted line: ideal Gaussian envelope). (c) Instantaneous RF frequency (solid line: linear fitting, circle: obtained from experimental result). (d) Compressed pulse by autocorrelation.

instantaneous microwave carrier frequencies within the main pulsewidth, calculated from the experimental result by Hilbert transform [30]. It is shown that a linearly increasing carrier frequency is obtained with a central frequency of 20.2 GHz and a positive chirp rate of 0.02 GHz/ps, which agree well with the theoretical predictions by (7). A linear fitting curve is also shown in Fig. 5(c) to illustrate the linear frequency chirping. According to the time-domain waveform and its carrier frequency distribution, the TBWP of the generated chirped microwave pulse is estimated to be around 44.8, which agrees well with the theoretically predicted TBWP of 49.4 by (8). Fig. 5(d) shows the compressed pulse with an FWHM of 21 ps, which is obtained by calculating the autocorrelation of the generated microwave pulse according to (9). By comparing the FWHMs of the waveforms in Figs. 5(b) and (d), a pulse compression ratio as large as 54.7 is obtained.

Then the tuning of the chirp profile is demonstrated. In the experiment, the Sagnac loop mirror with a reflection spectrum having an increasing FSR is also achieved when we choose the fiber loop to have a negative length difference of $\Delta L_0 = -11.3$ mm by tuning the TDL in the loop. A linearly chirped microwave pulse with a higher central frequency of 24.5 GHz and a negative chirp rate of $-0.022\ \mathrm{GHz/ps}$ is then experimentally generated after the wavelength-to-time mapping in the 30.8-km SMF. The experimental results are shown in Fig. 6. The TBWP of the generated chirped microwave pulse is estimated to be around 41, which is close to the value of the first generated chirped pulse. In fact, the TBWP is only determined by the parameters of the CFBG according to (8). Fig. 6(d) shows the autocorrelation result. A compression ratio of 56.5 is achieved. Compared with the autocorrelation result for a chirped microwave with the same chirp profile but an ideal Gaussian envelope, as shown in the inset of Fig. 6(d), although the width of the autocorrelation waveform is maintained unchanged, high-level sidelobes are observed in the experiment, which are resulted from the non-Gaussian-like envelope of the generated waveform. One possible solution to eliminate the autocorrelation sidelobes is to use a CFBG with a Gaussian-shape reflection spectrum, to ensure the spectrum of the shaped optical pulse to also have a Gaussian envelope, leading to the generation of a temporal waveform with a Gaussian envelope after the linear wavelength-to-time mapping.

IV. Conclusion

We have proposed and experimentally demonstrated a new approach to optically generating linearly chirped microwave pulses based on optical spectral shaping and linear wavelength-to-time mapping. The key component in the proposed system is the CFBG-incorporated Sagnac loop mirror, which has a spectral response with an increasing or decreasing FSR, employed to act as the optical spectral filter to shape the spectrum of the input ultrashort optical pulse. By using a linear dispersive element, such as a length of SMF in our experimental demonstration, to perform the linear wavelength-to-time mapping, a linearly chirped microwave pulse with a high central frequency and tunable chirp profile was generated. The proposed approach has the advantage of simpler design, which can find applications in high-speed communications and modern radar systems.

References

[1] D. K. Barton, *Radar System Analysis and Modeling*. Boston, MA: Artech House, 2005.
[2] H. D. Griffiths and W. J. Bradford, "Digital generation of high time-bandwidth product linear FM waveforms for radar altimeters," *IEE Proc.-F*, vol. 139, no. 2, pp. 160–169, Apr. 1992.
[3] H. Kwon and B. Kang, "Linear frequency modulation of voltage-controlled oscillator using delay-line feedback," *IEEE Microw. Wireless Compon. Lett.*, vol. 15, no. 6, pp. 431–433, Jun. 2005.

[4] A. M. Weiner, "Femtosecond pulse shaping using spatial light modulators," *Rev. Sci. Instrum.*, vol. 71, no. 5, pp. 1929–1960, 2000.
[5] Z. Jiang, D. E. Leaird, and A. M. Weiner, "Optical arbitrary waveform generation and characterization using spectral line-by-line control," *J. Lightw. Technol.*, vol. 24, pp. 2487–2494, 2006.
[6] M. Shen and R. A. Minasian, "Toward a high-speed arbitrary waveform generation by a novel photonic processing structure," *IEEE Photon. Technol. Lett.*, vol. 16, no. 4, pp. 1155–1157, Apr. 2004.
[7] R. E. Saperstien, N. Alic, D. Pasasenko, R. Rokitski, and Y. Fainman, "Time-domain waveform processing by chromatic dispersion for temporal shaping of optical pulses," *J. Opt. Soc. Am. B*, vol. 22, no. 11, pp. 2427–2436, 2005.
[8] J. Azaña, N. K. Berger, B. Levit, and B. Fischer, "Reconfigurable generation of high-repetition-rate optical pulse sequences based on time-domain phase-only filtering," *Opt. Lett.*, vol. 30, no. 23, pp. 3228–3230, 2005.
[9] J. Azaña, N. K. Berger, B. Levit, and B. Fischer, "Broadband arbitrary waveform generation based on microwave frequency upshifting in optical fibers," *J. Lightw. Technol.*, vol. 24, pp. 2663–2675, 2006.
[10] D. E. Leaird and A. M. Weiner, "Femtosecond direct space-to-time pulse shaping," *IEEE J. Quantum Electron.*, vol. 37, no. 4, pp. 494–504, Apr. 2001.
[11] J. D. McKinney, D. E. Leaird, and A. M. Weiner, "Millimeter-wave arbitrary waveform generation with a direct space-to-time pulse shaper," *Opt. Lett.*, vol. 27, no. 15, pp. 1345–1347, 2002.
[12] J. D. McKinney, D. Seo, D. E. Leaird, and A. M. Weiner, "Photonically assisted generation of arbitrary millimeter-wave and microwave electromagnetic waveforms via direct space-to-time optical pulse shaping," *J. Lightw. Technol.*, vol. 21, pp. 3020–3028, 2003.
[13] S. Xiao, J. D. McKinney, and A. M. Weiner, "Photonic microwave arbitrary waveform generation using a virtually-imaged phase-array (VIPA) direct space-to-time pulse shaper," *IEEE Photon. Technol. Lett.*, vol. 16, no. 8, pp. 1936–1938, Aug. 2004.
[14] D. E. Leaird and A. M. Weiner, "Femtosecond direct space-to-time pulse shaping in an integrated-optic configuration," *Opt. Lett.*, vol. 29, no. 13, pp. 1551–1553, 2004.
[15] A. Zeitouny, S. Stepanov, O. Levinson, and M. Horowitz, "Optical generation of linearly chirped microwave pulses using fiber Bragg gratings," *IEEE Photon. Technol. Lett.*, vol. 17, no. 3, pp. 660–662, Mar. 2005.
[16] M. A. Muriel, J. Azaña, and A. Carballar, "Real-time Fourier transformer based on fiber gratings," *Opt. Lett.*, vol. 24, no. 1, pp. 1–3, 1999.
[17] J. Azaña and M. A. Muriel, "Real-time optical spectrum analysis based on the time-space duality in chirped fiber gratings," *IEEE J. Quantum Electron.*, vol. 36, no. 5, pp. 517–526, May 2000.
[18] J. Azaña, L. R. Chen, M. A. Muriel, and P. W. E. Smith, "Experimental demonstration of real-time Fourier transformation using linearly chirped fiber Bragg gratings," *Electron. Lett.*, vol. 35, no. 25, pp. 2223–2224, 1999.
[19] B. Jalali, P. Kelkar, and V. Saxena, "Photonic arbitrary waveform generator," in *Proc. 14th Annu. Meeting IEEE Lasers Electro-Optics Soc.*, San Diego, CA, 2001, vol. 1, pp. 253–254.
[20] J. Chou, Y. Han, and B. Jalali, "Adaptive RF-photonic arbitrary waveform generator," *IEEE Photon. Technol. Lett.*, vol. 15, no. 4, pp. 581–583, Apr. 2003.
[21] I. Lin, J. D. McKinney, and A. M. Weiner, "Photonic synthesis of broadband microwave arbitrary waveforms applicable to ultra-wideband communication," *IEEE Microw. Wireless Compon. Lett.*, vol. 15, no. 4, pp. 226–228, Apr. 2005.
[22] H. Chi, F. Zeng, and J. P. Yao, "Photonic generation of microwave signals based on pulse shaping," *IEEE Photon. Technol. Lett.*, vol. 19, no. 9, pp. 668–670, May 2007.
[23] C. Wang, F. Zeng, and J. P. Yao, "All-fiber ultrawideband pulse generation based on spectral shaping and dispersion-induced frequency-to-time conversion," *IEEE Photon. Technol. Lett.*, vol. 19, no. 3, pp. 137–139, Feb. 2007.
[24] C. Wang and J. P. Yao, "Photonic generation of chirped millimeter-wave pulses based on nonlinear frequency-to-time mapping in a nonlinearly chirped fiber Bragg grating," *IEEE Trans. Microw. Theory Tech.*, vol. 56, no. 2, pp. 542–553, Feb. 2008.
[25] H. Chi and J. P. Yao, "Chirped RF pulse generation based on optical spectral shaping and wavelength-to-time mapping using a nonlinearly chirped fiber Bragg grating," *J. Lightw. Technol.*, vol. 26, pp. 1282–1287, 2008.
[26] H. Chi and J. P. Yao, "All-fiber chirped microwave pulse generation based on spectral shaping and wavelength-to-time conversion," *IEEE Trans. Microw. Theory Tech.*, vol. 55, no. 9, pp. 1958–1963, Sep. 2007.
[27] C. Wang and J. P. Yao, "Photonic generation of chirped microwave pulses using superimposed chirped fiber Bragg gratings," *IEEE Photon. Technol. Lett.*, vol. 20, no. 11, pp. 882–884, Jun. 2008.
[28] X. Shu, S. Jiang, and D. Huang, "Fiber grating Sagnac loop and its multiwavelength-laser application," *IEEE Photon. Technol. Lett.*, vol. 12, no. 8, pp. 980–982, Aug. 2000.
[29] G. P. Agrawal, *Nonlinear Fiber Optics*, 2nd ed. New York: Academic Press, 1995.
[30] S. Mallet, *A Wavelet Tour of Signal Processing*. San Diego, CA: Academic Press, 1999.

Chao Wang (S'08) received the B.Eng. degree in opto-electrical engineering from Tianjin University, Tianjin, China, in 2002, and the M.Sc. degree in optics from Nankai University, Tianjin, in 2005. Currently, he is working toward the Ph.D. degree in electrical engineering at the University of Ottawa, Ottawa, ON, Canada.

His current research interests include microwave signal generation, radio-over-fiber systems, fiber Bragg grating and their applications in microwave photonics systems.

Jianping Yao (M'99–SM'01) received the Ph.D. degree in electrical engineering from the Université de Toulon, Toulon, France, in 1997.

From 1999 to 2001, he held a faculty position with the School of Electrical and Electronic Engineering, Nanyang Technological University, Singapore. He holds a Yongqian Endowed Visiting Chair Professorship with Zhejiang University, China. He spent three months as an Invited Professor in the Institut National Polytechnique de Grenoble, France, in 2005. He joined the School of Information Technology and Engineering, University of Ottawa, Ontario, Canada, in 2001, where he is currently a Professor, Director of the Microwave Photonics Research Laboratory, and Director of the Ottawa-Carleton Institute for Electrical and Computer Engineering. His research has focused on microwave photonics, which includes all-optical microwave signal processing, photonic generation of microwave, millimeter wave and THz, radio over fiber, UWB over fiber, fiber Bragg gratings for microwave photonics applications, and optically controlled phased array antenna. His research interests also include fiber lasers, fiber-optic sensors and biophotonics. He has authored or coauthored more than 110 papers in refereed journals and over 100 papers in conference proceeding.

Dr. Yao is a registered professional engineer of Ontario. He is a member of SPIE, OSA, and a senior member of IEEE/LEOS and IEEE/MTT. He is an Associate Editor of the *International Journal of Microwave and Optical Technology*. He is on the Editorial Board of IEEE TRANSACTIONS ON MICROWAVE THEORY AND TECHNIQUES. Dr. Yao received the 2005 International Creative Research Award of the University of Ottawa. He was the recipient of the 2007 George S. Glinski Award for Excellence in Research. He was named University Research Chair in Microwave Photonics in 2007. He was a recipient of the NSERC Discovery Accelerator Supplements Award in 2008.